Properties of Celtic knot design of $p \times q$ square grid and $p \times q$ honeycomb grid

Yukari Funakoshi
yukarifunakoshi@gifu.shotoku.ac.jp
Faculty of Education, Gifu Shotoku Gakuen University, 501-6194, Japan

Megumi Hashizume
megumihashizume@math.akita-u.ac.jp
Faculty of Integrated science and Engineering for Environments,
Akita University, 010-8502, Japan

Abstract

Fisher-Mellor defined knotwork design as a type of alternating link diagram related to Celtic knots ([3]). In this paper, we define Celtic knot design (CKD) induced from $p \times q$ square grid and $p \times q$ honeycomb grid as a generalized knotwork design. We show the geometric properties of CKDs from these grids and present how these structures can be mathematically described and classified. These concepts and results support mathematics education by deepening understanding of geometric structures and work well with technology-enhanced instructional design ([4]).This multidisciplinary approach, integrating mathematics, art, culture, and technology, offers potential applications in STEAM education.

1 Introduction

The Celtic knot is a traditional geometric symbol of the Celtic peoples of ancient Britain, Scotland, and Ireland. It appears in [7] and in cultural works such as the Book of Kells, a bible manuscript decorated with many Celtic knots. P. R. Cromwell introduced the Celtic knot into knot theory ([1, 2]). In 2004, G. Fisher and B. Mellor showed results for "Celtic knot design induced from $p \times q$ square grid" ([3]). Our study presents results for *Celtic knot design* (*CKD*) induced from both $p \times q$ *square grid* and $p \times q$ *honeycomb grid*. Specifically, while Fisher and Mellor focused on the number of components in square grid-based designs, our study provides new results on the number of crossings, diagram shapes, component classification, and geometric properties of CKDs such as decomposition into substructures. We extend our results for the CKD induced from a $p \times q$ square grid by introducing CKD derived from $p \times q$ honeycomb grid.

In Section 2, we introduce basic definitions of knot theory and give key definitions of CKD, $p \times q$ square grid, $p \times q$ honeycomb grid, spur, track, etc. We also show known results and some of our own. In Section 3, we show main results of the CKD induced from a $p \times q$ square grid and a $p \times q$

honeycomb grid (Proposition 3.2, Theorem 3.14, Theorem 3.15, Theorem 3.16, Proposition 3.21, Theorem 3.22, Corollary 3.23, Theorem 3.28, and Proposition 3.29). Results of the CKD induced from a $p \times q$ honeycomb grid correspond to results of the CKD induced from a $p \times q$ square grid. For example, results on the number of components of the links represented by CKDs are shown in Theorem 2.9 ([3]) and Theorem 3.15, and results on the shape of CKDs are shown in Proposition 3.1, Proposition 3.2, Theorem 3.22, Corollary 3.23, and Proposition 3.24.

Programming education has become more popular around the world in recent years. As of 2024, about two-thirds of countries offer some form of computing education in their school curricula, growing fast in Africa, Asia, and Latin America [10]. In this context, Japan introduced mandatory programming education in elementary schools in 2020. The animations developed by Y. Funakoshi [4] for constructing Celtic knot projections based on $p \times q$ square and honeycomb grids not only support mathematical education, but also serve as effective tools for programming education. These constructions can be implemented algorithmically, allowing students to engage with computational logic, geometric reasoning, and visual creativity. By integrating mathematical structure, algorithmic thinking, and artistic design, CKDs provide a rich interdisciplinary platform for STEAM education. These visual constructions enable exploration of symmetry, pattern generation, and cultural narratives, which align closely with its educational, creative, and integrative goals [11].

2 Preliminaries

2.1 Terminologies in Knot Theory

Definition 2.1 (component, link, knot)**.** An *r-component link* is a union of r disjoint smooth embeddings of S^1 into $\mathbb{R}^3$. Each image of S^1 is called a *component* of the link. A 1-component link is called a *knot*.

Definition 2.2 (projection, diagram, component segment set, crossing, trivial)**.** Let $p : \mathbb{R}^3 \to \mathbb{R}^2$ be a projection and L be a link in $\mathbb{R}^3$. If all multiple points of $p(L)$ are transverse double points, then $p(L)$ is called a *projection* of L. A *diagram* of L is a projection with over/under information at each double point. A diagram of a knot is called a *knot diagram*. The union of segments composing a diagram that corresponding to a component of L is called the *component segment set*. A point in a diagram of L corresponding to the double point in $p(L)$ is called a *crossing*. A *self crossing* is a crossing on a single component. A knot is *trivial* if it admits a diagram with no crossings.

On the other hand, a projection may be regarded as obtained from a diagram by ignoring the over/under information of the crossings.

Definition 2.3 (alternating)**.** Fix a base point on each component segment set of a diagram of a link and travel along it. The diagram is *alternating* if the crossings alternate over and under along each component segment set. A link is *alternating* if it admits an alternating diagram.

Definition 2.4 (plane ambient isotopy)**.** For a projection of a link, an ambient isotopy in $\mathbb{R}^2$ is called *plane ambient isotopy*. For projections P_1, P_2 of a link, suppose that P_1 is plane ambient isotopic to P_2. Moreover, for diagrams D_1, D_2 of the link, if P_1 (P_2 respectively) is obtained from D_1 (D_2 respectively), then we say that D_1 is plane ambient isotopic to D_2 as in Figure 1.

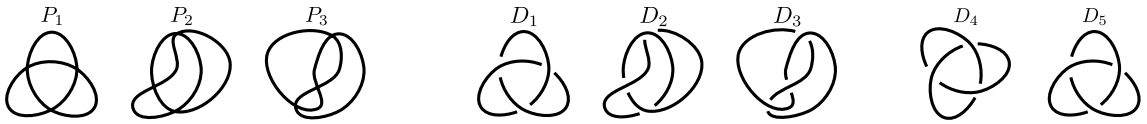

Figure 1: P_1 is plane ambient isotopic to P_2, and D_1 is plane ambient isotopic to D_2, D_4, and D_5. However, P_1 is not plane ambient isotopic to P_3, nor is D_1 to D_3.

For diagrams A, B, if B is obtained from A by parallel translation in $\mathbb{R}^2$, then we denote $A \parallel B$. For example, $D_1 \parallel D_5$ and $D_1 \nparallel D_i$ $(i = 2, 3, 4)$ as in Figure 1. For the definitions of other standard terms in knot theory, we refer to "A Survey of Knot Theory" ([6]).

2.2 Definition of Celtic knot design and its known results

Definition 2.5 (grid)**.** A closed subset of a tiled $\mathbb{R}^2$ whose boundary consisting of some edges of the polygons is called a *grid*. For a grid G, the boundary of G is denoted by ∂G.

Definition 2.6 (Celtic knot projection, Celtic knot design)**.** Draw a new polygon inscribed at the midpoints of the edges for any polygon forming a grid. Then the union of the new polygons is considered a projection of a link. The projection is called *Celtic knot projection* (*CKP*). A diagram obtained from the CKP by adding alternating over/under information for each double point is called *Celtic knot design* (*CKD*).

Note that a CKD may represent either a knot or a multi-component link. In this paper, we use the term CKD to denote diagrams representing the corresponding link. To align with our definitions, we redefine $p \times q$ *knotwork panel* ([3]) as follows:

Definition 2.7 ($p \times q$ square grid)**.** Let $p, q \in \mathbb{N}$ with $p \leq q$. We say that a grid is the $p \times q$ *square grid* if the grid is arranged by $p \times q$ squares vertically and horizontally on an orthogonal coordinate system, where the length of a square composing the grid is 1 as (a) in Figure 4.

In general, a diagram is obtained from a link. In this paper, a CKD defines the link. A CKD varies depending on how it is added over/under information for any double point of a CKP.

Remark 2.8. Any grid has two CKDs.

These two CKDs are mirror images of each other as (a) or (b) in Figure 2. In this paper, we fix the over/under information for any crossing as in Figure 3.

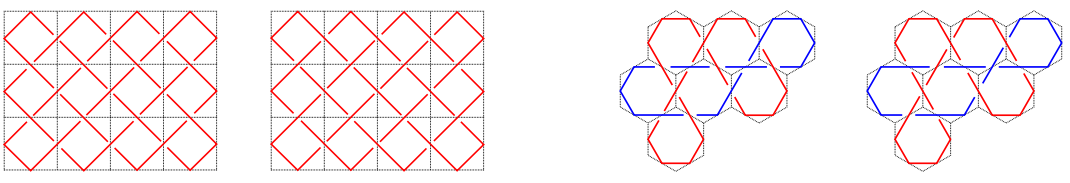

Figure 2: There are two CKDs for each grid.

Figure 3: The over/under information of the crossing on an edge of a polygon of a grid

Let G be a $p \times q$ square grid and D be the CKD induced from G as (b) in Figure 4. For any component segment set of D, a knot diagram is obtained by ignoring the over/under information of the crossings except for the self crossings. Then, $\mathcal{K}_D^\sharp$ denotes the set of the knot diagrams. In this paper, each component segment set is colored by one color, and two different component segment sets are colored by different colors. The element of $\mathcal{K}_D^\sharp$ formed from a component segment set is colored to match the set. Let $r = gcd(p, q)$, $p' = \frac{p}{r}$, and $q' = \frac{q}{r}$.

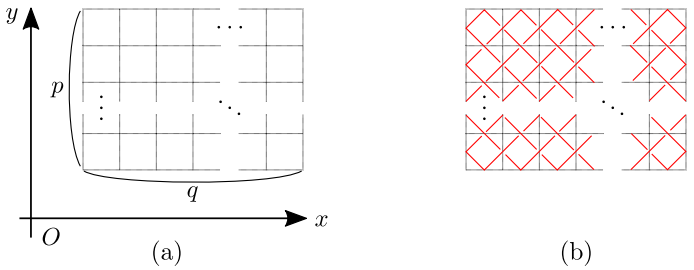

Figure 4: The $p \times q$ square grid and the CKD induced from the grid

Theorem 2.9 ([3]). *A CKD induced from a $p \times q$ square grid represents an r-component link.*

Since p' and q' are relatively prime numbers, we have;

Corollary 2.10. *The CKD induced from the $p' \times q'$ square grid is a knot diagram.*

Let P be a projection obtained from an element of $\mathcal{K}_D^\sharp$. Then, P consists of the line segments, where each line segment has slope 1 or -1 on the orthogonal coordinate system and the end points of each line segment are on ∂G.

Claim 2.11. *The projection P intersects on the left and the right sides of ∂G at p' points each, and P intersects on the upper and the lower sides of ∂G at q' points each.*

Proof. Let the base point be the top intersection of P and the left side of ∂G. We travel on P clockwise from the base point to the same point. Let $k, \ell \in \mathbb{N}$ be the numbers of vertical and horizontal roundtrips, respectively. Based on the slopes of the segments and the shape of G, $2pk = 2q\ell$ holds. Let $(k, \ell) \in \mathbb{N}^2$ be the minimal solution to the equation. Then, $pk = q\ell = lcm(p, q)$ holds. Furthermore, this fact together with $pq = lcm(p, q)gcd(p, q) = lcm(p, q)r$ shows that $\ell = \frac{p}{r} = p'$, $k = \frac{q}{r} = q'$. Hence, P intersects on the left and the right sides of ∂G at p' points each, and P intersects on the upper and the lower sides of ∂G at q' points each. □

Moreover, Fisher and Mellor claimed that any element of $\mathcal{K}_D^\sharp$ is plane ambient isotopic to the CKD induced from the $p' \times q'$ square grid ([3]). We show own proof of this claim as Theorem 3.5 in Section 3.1.

Example 2.12. Let D be the CKD induced from the 6×9 square grid. $K_i \in \mathcal{K}_D^\sharp$ $(i = 1, 2, 3)$ is plane ambient isotopic to the CKD induced from the $\frac{6}{3} \times \frac{9}{3}$ square grid in Figure 5.

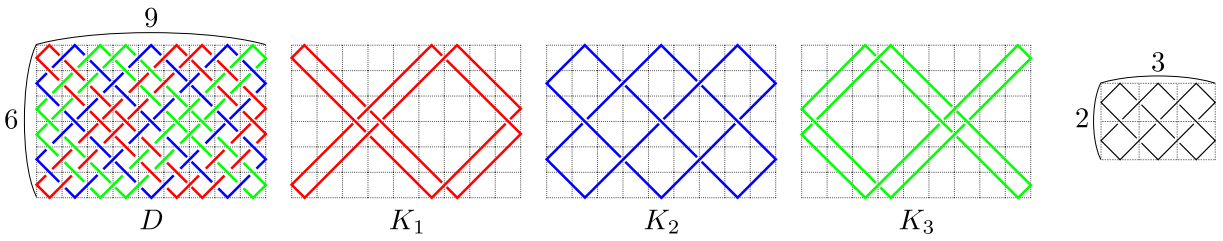

Figure 5: A relationship between the CKDs induced from the 6×9 and the 2×3 square grid

2.3 Celtic knot design of $p \times q$ honeycomb grid

Definition 2.13 ($p \times q$ honeycomb grid)**.** Let $p, q \in \mathbb{N}$ with $p \leq q$. We consider an oblique coordinate system with an angle of $\frac{\pi}{3}$ rad on the plane. Let $A = \{(x, y) \in \mathbb{R}^2 | 1 \leq x \leq q, 1 \leq y \leq p, x, y \in \mathbb{N}\}$. For any $(x, y) \in A$, draw a regular hexagon centered at (x, y) with side length $\frac{1}{\sqrt{3}}$ as in Figure 6. The union of the $p \times q$ regular hexagons is called the $p \times q$ *honeycomb grid*, and each hexagon with central coordinate (x, y) is simply denoted by (x, y).

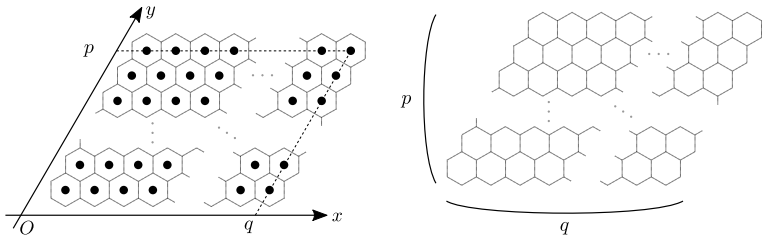

Figure 6: A black dot in the left figure represents the point $(x, y) \in A$ as the center of a regular hexagon that contains itself, and the right figure represents the $p \times q$ honeycomb grid.

Let G be a $p \times q$ honeycomb grid and D be the CKD induced from G. For a hexagon (m, n) composing G, let $(m, n)_1, \ldots, (m, n)_6$ be the midpoints of the edges of (m, n) ordered as in Figure 7. We may express to "the spur passes through $(1, n)_1$ ($(m, 1)_4$, $(q, n)_4$, $(m, p)_1$ respectively)" as "the spur passes through the regular hexagon in the leftmost column (the bottom row, the rightmost column, top row respectively) of G".

For any component segment set of D, a knot diagram is obtained by ignoring the over/under information of non-self crossings. Then, $\mathcal{K}_D^*$ denotes the set of the knot diagrams.

Definition 2.14 (spur)**.** We say that an element of $\mathcal{K}_D^*$ is the *spur* of D if the element passes through the point $(1, p)_1$.

Definition 2.15 (track)**.** The set of elements of $\mathcal{K}_D^*$ other than the spur is called the *track* of D.

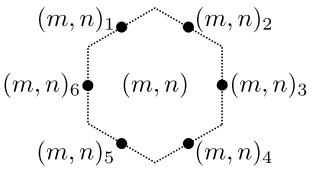

Figure 7: The black dots represent the midpoints of the edges of (m,n).

Example 2.16. Let D be the CKD induced from the 7×11 honeycomb grid. The spur and the elements of the track of D are as in Figure 8.

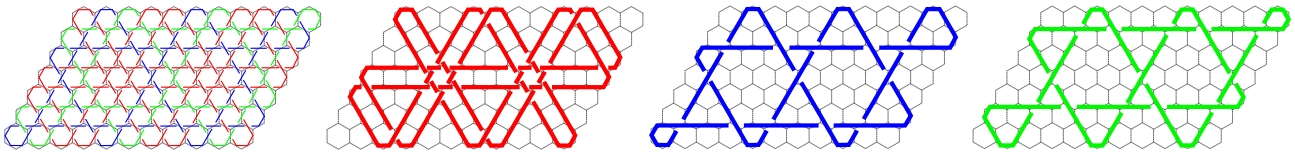

Figure 8: K_1 is the spur of D and K_2, K_3 are the elements of the track of D.

In this paper, each component segment set is colored by one color, and two different component segment sets are colored by different colors. The element of $\mathcal{K}_D^*$ formed by a component segment set is colored the same color as the component segment set. In particular, the spur is depicted in red.

Fact 2.17. *For any $p \times q$ honeycomb grid G, the spur bends only at ∂G as in Figure 9.*

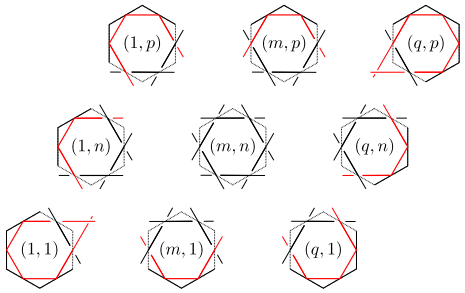

Figure 9: $m \neq 1, q$ and $n \neq 1, p$.

Let the base point O be the point of the spur at $(1,p)_1$ as in Figure 10. We travel on the spur clockwise from O.

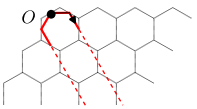

Figure 10: The travel on the spur from the base point O

Theorem 2.18. *The spur of D passes through $(q,1)_4$.*

Proof. We begin traveling clockwise on the spur from O, move toward the lower right, and return to O in the direction toward the upper left. Let $m', n' \in \mathbb{N}$ with $2 \leq m' \leq q$, $1 \leq n' \leq p-1$. By Fact 2.17, it is only at $(m',1)_4$, $(q,n')_4$ that the spur may bend toward the upper left direction. Before we pass through $(m',1)_4$, $(q,n')_4$ $(m' \neq q,\ n' \neq 1)$ toward the upper left direction, the direction of this travel changes toward upper left at least once. Then, the direction of the travel changes to upper left for the first time at $(q,1)_4$. Hence, the spur passes through $(q,1)_4$ as in Figure 11.

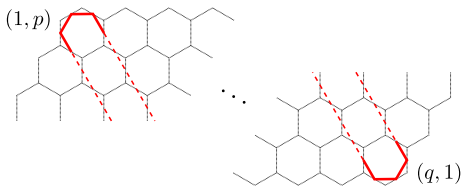

Figure 11: The spur of D passes through $(q,1)_4$.

□

3 Main results

3.1 Results of Celtic knot design of $p \times q$ square grid

Let G be a $p \times q$ square grid and D be the CKD induced from G. Let $\mathcal{K}^\sharp_D$ be as in Section 2.2. Let $r = gcd(p,q)$, $p' = \frac{p}{r}$ and $q' = \frac{q}{r}$. For $1 \leq i \leq p', 1 \leq j \leq q'$, let $G(i,j)$ be a closure of a piece of G obtained by dividing G into $p'q'$ pieces where the closure is the $r \times r$ square grid and the closure is located i-th from the top and j-th from the left on G.

Proposition 3.1. *The crossings of D on $\partial G(i,j)$s are the self crossings.*

The proof of Proposition 3.1 is given together with that of Proposition 3.2.

For any i, j, take a small disk at any crossing on $\partial G(i,j)$, and let $D(i,j)$ be the diagram on $G(i,j)$ obtained by replacing the small disks as in Figure 12. Then, any $D(i,j)$ is alternating by Definition 2.6. Thus, any $D(i,j)$ is regarded as the CKD induced from $G(i,j)$.

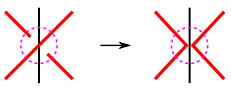

Figure 12: The deformation for obtaining $D(i,j)$s from D

For $1 \leq k \leq r$, let $e_k \in \mathcal{K}^\sharp_{D(1,1)}$ that has the k-th intersection from the top on the left side of $\partial G(1,1)$. Let $D(1,1)^{\frac{\pi}{2}}$ be the image of $D(1,1)$ rotated by $\frac{\pi}{2}$ rad on $G(1,1)$. Then, e_k is transformed into the k-th element from the left that passes through the lower side of $\partial G(1,1)$.

Proposition 3.2. *If $i+j$ is even, then $D(i,j) \parallel D(1,1)$. If $i+j$ is odd, then $D(i,j) \parallel D(1,1)^{\frac{\pi}{2}}$.*

Proof. Let P be a projection obtained from an element of $\mathcal{K}_D^\sharp$. P has at least one intersection with each side of ∂G by Claim 2.11. Let the base point be the top intersection on the left side of ∂G. We travel on P clockwise from the base point to the same point. For simplicity, we may call the travel P.

First, we divide P into the parts from the left side to the right side of ∂G and from the right side to the left side of ∂G.

bL-R: The part of P that starts from the base point on the left side of ∂G and reaches the right side of ∂G

The base point of P is on $G(h,1)$ where $1 \leq h \leq p'$. Let $k \in \mathbb{N}$ such that P starts from the base point in the k-th square from the top left square of $G(h,1)$ as in Figure 13, where $1 \leq k \leq r$. If $h = 1$, P is reflected by the upper side of $\partial G(1,1)$. If $1 < h$, P passes through the upper side of $\partial G(h,1)$. Then, the intersections of $\partial G(i,j)$ and P as in Figures 14 and 15 are determined by the slopes of the line segments composing P. (a)$^\mathrm{b}$ ((e)$^\mathrm{b}$ respectively) in Figure 13 corresponds to (a) ((e) respectively) in Figure 14. Thus, the part bL-R starts from (a) or (e).

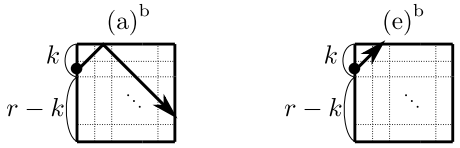

Figure 13: Each dot represents the base point on $G(h,1)$, and each arrow represents the line segments with the direction of the travel on $G(h,1)$.

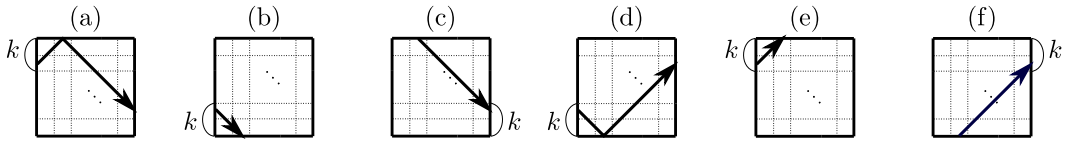

Figure 14: The part bL-R or a part L-R consists of the arrows, where each arrow represents the line segments with the direction of the travel on $G(i,j)$.

case (a): P passes through (a) in Figure 14

Step 1. If P reaches the right side of ∂G by (a), the part bL-R is finished. If P goes straight after (a), then P repeats (b), (c) in this order, P goes into (d) after repeating (b), (c), or P goes into (d) directly. When P reaches the right side of ∂G via (c), the part bL-R is finished. When P is reflected by the lower side of ∂G via (d), we go to Step 2.

Step 2. If P reaches the right side of ∂G via (d), the part bL-R is finished. If P goes straight after (d), then P repeats (e), (f) in this order, P goes into (a) after repeating (e), (f), or P goes into (a) directly. When P reaches the right side of ∂G via (f), the part bL-R is finished. When P is reflected by the upper side of ∂G via (a), we go to Step 1.

case (e): P passes through (e) in Figure 14

P is reflected by the upper side of ∂G via (a) after repeating (e), (f) in this order since $p' \leq q'$. We go to Step 1 in case (a).

Hence, the part bL-R is finished at (a), (c), (d) or (f) in Figure 14. Then, a part R-L starts from (g), (h), (j) or (k) in Figure 15.

R-L: A part of P that starts from the right side of ∂G and reaches the left side of ∂G

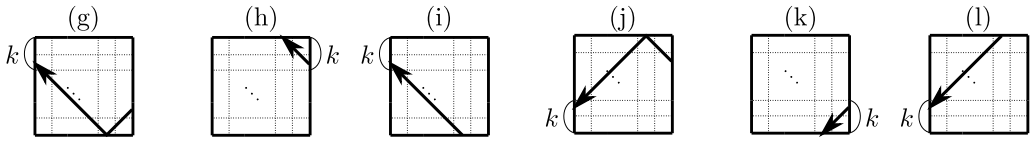

Figure 15: A part R-L consists of the arrows, where each arrow represents the line segments with the direction of the travel on $G(i, j)$.

By similar arguments of the part bL-R, a part R-L is finished at (g), (i), (j) or (l) in Figure 15. If a part R-L is finished at $G(h, 1)$, P is finished at (g) or (i). Otherwise, a part L-R starts from (a), (b), (d) or (e) in Figure 14.

L-R: A part of P that starts from the left side of ∂G and reaches the right side of ∂G

By similar arguments of the part bL-R, a part L-R is finished at (a), (c), (d) or (f) in Figure 14. Then, a part R-L starts again.

By the above argument, the connections obtained from the travel on P between the figures in Figure 14 and Figure 15 are illustrated by the arrows as in Figure 16.

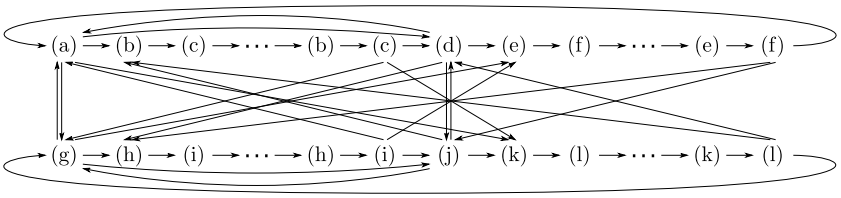

Figure 16: (a) $\to$ (b) represents that P passes through $G(i, j)$ by (b) after (a).

Next, for any $G(i, j)$ that P passes through, we consider the parity of $i + j$. P passes through $G(i - 1, j)$, $G(i + 1, j)$, $G(i, j - 1)$ or $G(i, j + 1)$ after $G(i, j)$. For i, j, the numbers $(i - 1) + j$, $(i + 1) + j$, $i + (j - 1)$ and $i + (j - 1)$ have the same parity, and have the different parity from $i + j$. This fact together with the connections between the figures in Figure 14 and Figure 15 shows that a connected pair of one of (a)-(f) and one of (g)-(l) in Figure 16 has the same parity. Moreover, a connected pair of (a)-(f) or a connected pair of (g)-(l) in Figure 16 has the different parities. Hence, (a)-(f) and (g)-(l) are classified into two sets based on the parity of $i + j$: (a), (c), (e), (g), (i), and (k) belong to one set, while (b), (d), (f), (h), (j), and (l) belong to the other set.

Finally, we focus on the shape of the union of the line segments composing P on any $G(i, j)$ which P passes through. By the previous argument, for $1 \leq i \leq p', 1 \leq j \leq q'$, the union on $G(i, j)$ consists of figures belonging to one of the two classified sets. Then, the union is a subset of the rectangle. The perimeter of the rectangle is $2\sqrt{2}r$. On the other hand, recall that the length of P is $2\sqrt{2}p'q'r$ by Claim 2.11, and G is divided into $p'q'$ $G(i, j)$s. Thus, the union is the rectangle.

Any double point of P is on $\bigcup \partial G(i,j)$. Hence, any crossing of an element of $\mathcal{K}_D^\sharp$ is on $\bigcup \partial G(i,j)$s. Therefore, Proposition 3.1 is proved. Since Theorem 2.9 and the fact that the union of the line segments composing P is the rectangle on any $G(i,j)$, there are r rectangles on any $G(i,j)$, where any two rectangles on $G(i,j)$ are formed by two projections obtained from mutually different elements of $\mathcal{K}_D^\sharp$. Then, for any pair of i,j, the union of the rectangles on $G(i,j)$ is regarded as the CKP obtained from $G(i,j)$. On the other hand, the rectangles formed by P on $G(i,j)$ with even and odd values of $i+j$ are $\frac{\pi}{2}$-rotationally symmetric to each other. Then, the CKPs obtained from $G(i,j)$ with even and odd values of $i+j$ are also $\frac{\pi}{2}$-rotationally symmetric. Hence, $D(i,j)$s with even and odd values of $i+j$ are also $\frac{\pi}{2}$-rotationally symmetric, by Definition 2.6. Then, Proposition 3.2 holds by the parity of $1+1$. □

Corollary 3.3. *The number of $D(i,j)$s with $D(i,j) \parallel D(1,1)$ is $\lceil \frac{p'}{2} \rceil \lceil \frac{q'}{2} \rceil + \lfloor \frac{p'}{2} \rfloor \lfloor \frac{q'}{2} \rfloor$, and the number of $D(i,j)$s with $D(i,j) \parallel D(1,1)^{\frac{\pi}{2}}$ is $\lceil \frac{p'}{2} \rceil \lfloor \frac{q'}{2} \rfloor + \lfloor \frac{p'}{2} \rfloor \lceil \frac{q'}{2} \rceil$.*

Example 3.4. Let $D_{6\times 9}$ be the CKD induced from the 6×9 square grid. The number of $D(i,j)$s with $D(i,j) \parallel D(1,1)$ is 3, and $D(i,j)$s with $D(i,j) \parallel D(1,1)^{\frac{\pi}{2}}$ is 3 as in Figure 17.

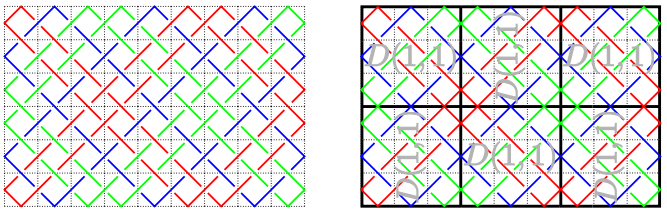

Figure 17: $D_{6\times 9}$ and the arrangement of $D(1,1)$s and $D(1,1)^{\frac{\pi}{2}}$s on $D_{6\times 9}$

We provide our own proof of the claim by Fisher and Mellor, which was mentioned in Section 2.2.

Theorem 3.5 ([3])**.** *Any element of $\mathcal{K}_D^\sharp$ is plane ambient isotopic to the CKD induced from the $p' \times q'$ square grid.*

Proof. First, we compare P obtained from an element of $\mathcal{K}_D^\sharp$ and the CKP obtained from the $p' \times q'$ square grid. Each of the left and right sides (the upper and lower sides respectively) of ∂G is divided into p' (q' respectively) equal parts of length r. Then, take the midpoint for any part. Connect each midpoint on the left or lower (left or upper respectively) sides of ∂G to the midpoint on the right or upper (right or lower respectively) sides of ∂G by the line segment of slope 1 (-1 respectively). The union of the line segments is regarded as a projection of a link, since each midpoint is connected by line segments of slopes 1 and -1. The projection, denoted by P', is the enlarged r times figure of the CKP obtained from the $p' \times q'$ square grid. By the above argument and Proposition 3.2, each of $2(p'+q')$ equal parts of ∂G contains one point of P and one point of P'. The line segments connected to each midpoint are kept fixed with the slopes preserved, while each point of P' is moved to coincide with the corresponding point of P. Then, P' and P coincide as projections. Hence P is plane ambient isotopic to the CKP obtained from the $p' \times q'$ square grid.

Next, we focus on the over/under information of a crossing. Let $K \in \mathcal{K}_D^\sharp$ that obtains P. P divides G into rectangles and triangles. For any polygon of P, each vertex on ∂G doesn't correspond

to a crossing of K, and each vertex on the interior of G corresponds to a crossing of K. Take the checkerboard coloring for K where the top crossing of K on a shaded region is on a horizontal edge of G. Then, regions of K corresponding to some rectangles of P are shaded, and a region of K corresponding to any triangle of P is not shaded. By the following mention of Remark 2.8, the coloring at a neighborhood of any crossing of K is as in Figure 18. On the other hand, for the CKD induced from the $p' \times q'$ square grid, take the same checkerboard coloring as the above. By the same argument as the above, the coloring at a neighborhood of any crossing of the CKD induced from the $p' \times q'$ square grid is as in Figure 18. Since P is plane ambient isotopic to the CKP obtained from the $p' \times q'$ square grid, over/under information of the top or bottom (the left or right respectively) crossing on a shaded region of K and the top or bottom (the left or right respectively) crossing on a shaded region of the CKD induced from the $p' \times q'$ square grid are the same. Therefore, any element of $\mathcal{K}_D^\sharp$ is plane ambient isotopic to the CKD induced from the $p' \times q'$ square grid. □

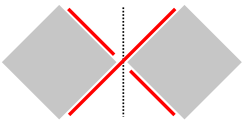

Figure 18: The over/under information of the crossing on an edge of a polygon of G, and the checkerboard coloring of a neighborhood of the crossing

Corollary 3.6. *Any element of $\mathcal{K}_D^\sharp$ is alternating.*

In general, *the crossing number* of a link is defined as the minimum number of crossings among all possible diagrams of the link. On the other hand, Lemma 3.7 and Proposition 3.8 present results for the number of crossings in a specific diagram, which is different from the crossing number.

Lemma 3.7. *D has $2pq - p - q$ crossings.*

Proof. By Definition 2.7, the cardinality of the set of the sides of the squares composing G without ∂G is $2pq - p - q$. Moreover, for any element of the set, there exists a crossing of D on the midpoint of the element by Definition 2.6. Hence, D has $2pq - p - q$ crossings. □

Proposition 3.8. *Any element of $\mathcal{K}_D^\sharp$ has $2p'q' - p' - q'$ crossings.*

Proof. It follows from Theorem 3.5 and Lemma 3.7. □

Remark 3.9. Kauffman, Murasugi and Thistlethwaite showed that if a link L admits an alternating, irreducible diagram of m crossings, then L cannot be projected with fewer than m crossings ([5, 8, 9]). This fact together with Proposition 3.8 shows that the minimal number of the crossings of any diagram of the knot represented any element of $\mathcal{K}_D^\sharp$ is $2p'q' - p' - q'$ except for the CKD induced from a $p \times np$ square grid.

3.2 Results of Celtic knot design of $p \times q$ honeycomb grid

For a $p \times q$ honeycomb grid G, let (m, n), $(m, n)_i$ $(i = 1, 2 \ldots, 6)$, D, $\mathcal{K}_D^*$ and O be as in Section 2.3. The spur of D passes through at least one reglar hexagon in the rightmost column of G by Theorem 2.18. Let (q, s) be the top regular hexagon that the spur passes through in the rightmost column of G as in Figure 19, and let $r := p - s + 1$.

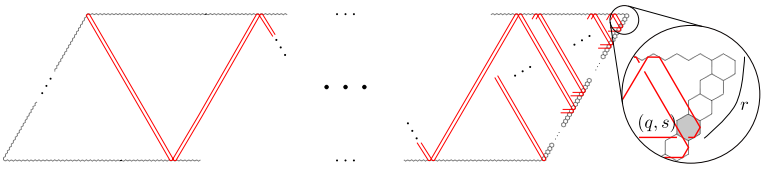

Figure 19: The shaded hexagon represents (q, s).

For $r \geq 2$, $k \in \mathbb{N}$ $(1 \leq k \leq r - 1)$, let $T_k \in \mathcal{K}_D^*$ passing through $(q, p - r + 1 + k)_4$ and $L := \{\text{the spur}, T_k\}$.

Lemma 3.10. *Any pair of elements of L are different elements of $\mathcal{K}_D^*$.*

Proof. Since the spur passes through $(q, p - r + 1)_4$, if $r \geq 2$, then T_k is not the spur. Let $i, j \in \mathbb{N}$ where $1 \leq i \leq \frac{q+1}{r+1}$, $1 \leq j \leq \frac{p+1}{r+1}$. We travel on all of T_k simultaneously counterclockwise from $(q, p - r + 1 + k)_4$. By Definitions 2.6 and 2.13, for any i, j, all of T_k simultaneously pass through $(1, (j-1)(r+1)+k)_1$ on ∂G. Similarly, all of T_k simultaneously pass through $((i-1)(r+1)+k, 1)_4$, $(q, (j-1)(r+1)+1+k)_4$, $((i-1)(r+1)+1+k, p)_1$ on ∂G. Then, the mutual positional relation of any pair of T_k is not deviated during the travels. Hence, all of T_k are different elements. Therefore, any pair of elements of L are different elements. □

By the definition of r and Lemma 3.10, Proposition 3.11 holds.

Proposition 3.11. *For $p \in \mathbb{N}$, if $q = p$, then the spur of D has no self crossing and each element of the track of D has one self crossing.*

We travel clockwise from O to O via $(q, 1)_4$ on G by Theorem 2.18. The travel from O to $(q, 1)_4$ is called the first half travel. The travel from $(q, 1)_4$ to O is called the second half travel. Let S_1 (S_2 respectively) be the subset of the projection obtained from the spur corresponding to the first half travel (the second half travel respectively), with over/under information added to the crossings that are passed through twice during the half travel.

Lemma 3.12. *If the spur traverses $(q, 1)$ clockwise, then S_2 passes through the regular hexagons left or lower adjacent to the regular hexagons which S_1 passes through.*

Proof. We consider the travel on S_1 that starts from O clockwise, and the travel on S_2 that starts from O counterclockwise simultaneously. Note that, the direction of the travel in this proof on S_2 is opposite of the direction of the second half travel. Let $i, j \in \mathbb{N}$ where $1 \leq i \leq \frac{q+1}{r+1}$, $1 \leq j \leq \frac{p+1}{r+1}$. By a similar argument of the proof of Lemma 3.10, S_1 passes through $(1, j(r + 1))_1$ and S_2 passes through $(1, j(r + 1) - 1)_1$ simultaneously. If $j = \frac{p+1}{r+1}$, $(1, j(r + 1))_1$ is not defined. In this case,

S_1 passes through $(1,p)_1$. S_1 passes through $(i(r+1),1)_4$ and S_2 passes through $(i(r+1)-1,1)_4$ simultaneously. If $i=\frac{q+1}{r+1}$, $(i(r+1),1)_4$ is not defined. In this case, S_1 passes through $(q,1)_4$. S_1 passes through $(q,(j-1)(r+1)+1)_4$ and S_2 passes through $(q,(j-1)(r+1))_4$ simultaneously. If $j=1$, $(q,(j-1)(r+1))_4$ is not defined. In this case, S_2 passes through $(q,1)_4$. S_1 passes through $((i-1)(r+1)+1,p)_1$ and S_2 passes through $((i-1)(r+1),p)_1$ simultaneously. If $i=1$, $((i-1)(r+1),p)_1$ is not defined. In this case, S_2 passes through $(1,p)_1$. Then, S_1 and S_2 are parallel during the travels except for $(1,p)$ and $(q,1)$ since S_1 and S_2 are closed at $(1,p)_1$ and $(q,1)_4$. □

Definition 3.13 (broken segment, length of a broken segment)**.** Let P_K be a projection obtained from $K\in\mathcal{K}_D^*$. A subset of a line segment composing P_K which has just two points intersecting with ∂G is called a *broken segment (of K)*. The *length of a broken segment* is the distance between the two intersections.

Theorem 3.14. *If the spur of D traverses $(q,1)$ counterclockwise, then D is a knot diagram.*

Proof. Let (m_e,p) be the e-th regular hexagon in the top row of G which the spur passes through during the travel from O to O. By $O=(1,p)_1$, $(m_1,p)=(1,p)$ holds. Let b_e be the number of the regular hexagons in the top row of G from (q,p) to (m_e,p). If $e=1$, then $b_1=q\geq p$. Thus, $1\leq b_e\leq q$ and $m_e=q-b_e+1$ hold. Then, there are three cases.

Assume $b_1=q=p$. The spur traverses $(q,1)=(p,1)$ clockwise by Proposition 3.11.

Assume $b_1=q=p+1$. The spur traverses $(q,1)=(p+1,1)$ counterclockwise. Then, S_2 passes through p hexagons in the top row of G $(2,p),\ldots,(p+1,p)$ in this order, that is, $b_e=p-e+2$, $(e=2,3,\ldots,p+1)$.

Assume $b_1=q\geq p+2$. Then $b_2=b_1-p-1$ holds. Moreover, suppose that $e\geq 2$. If $b_e\geq p+2$, then $b_{e+1}=b_e-p-1$. If $b_e=p+1$, then the spur traverses $(q,1)$ counterclockwise. If $b_e=p$, then the spur traverses $(q,1)$ clockwise. If $b_e\leq p-1$, then $b_{e+1}=q-p+b_e$. Hence, it is enough to consider this case $b_e=p+1$.

We may suppose that the spur passes through $(1,p)_1$ ($(q,1)_4$ respectively) in S_1 (S_2 respectively). Let u_1 (u_2 respectively) be the number of the regular hexagons in the top row of G that S_1 (S_2 respectively) passes through. Let v_1 (v_2 respectively) be the number of the regular hexagons in the rightmost column of G that S_1 (S_2 respectively) passes through. Recall that G is on the oblique coordinate. By Definition 3.13, S_1 and S_2 consist of broken segments. Focus on the broken segments with the directions composing the first half travel S_1 such that the direction of each broken segment corresponds to the positive direction of the x-axis. By the sum of the lengths of the broken segments, $(p+1)u_1-v_1=q(v_1+1)\Leftrightarrow -(p+1)u_1+(q+1)(v_1+1)=1\Leftrightarrow u_1=\frac{(q+1)(v_1+1)-1}{p+1}$ holds. Since $u_1,v_1\in\mathbb{N}$, $gcd(p+1,q+1)=1$ holds. Focus on the broken segments with the directions composing the second half travel S_2 such that the direction of each broken segment corresponds to the negative direction of the x-axis. By the sum of the lengths of the broken segments, $(p+1)(u_2+1)-(v_2+1)=qv_2$ $\Leftrightarrow u_2+1=\frac{(q+1)(v_1+v_2+1)}{p+1}-\frac{(q+1)(v_1+1)-1}{p+1}\Leftrightarrow u_2+1=\frac{(q+1)(v_1+v_2+1)}{p+1}-u_1$ holds. Since $u_2+1\in\mathbb{N}$ and $u_1\in\mathbb{N}$, $\frac{(q+1)(v_1+v_2+1)}{p+1}\in\mathbb{N}$ holds. By these arguments, since $gcd(p+1,q+1)=1$ and $v_1+v_2\leq p$, $\frac{(q+1)(v_1+v_2+1)}{p+1}\in\mathbb{N}\Leftrightarrow v_1+v_2=p$ holds. Suppose that the track is not empty. There is at least one regular hexagon that an element of the track passes through in the leftmost column of G by Definitions 2.6, 2.13 and a similar argument of the proof of Theorem 2.18. The same is true for regular hexagons in the bottom row, the rightmost column and the top row of G. This fact together

with the above argument shows that if the spur of D traverses $(q, 1)$ counterclockwise, then D is a knot diagram. □

Theorem 3.15. *D represents an r-component link.*

Proof. We prove $L = \mathcal{K}_D^*$ by dividing r into two cases.
Case 1: $r \geq 2$
There is at least one element of $\mathcal{K}_D^*$ which is not the spur. Let $i, j, k \in \mathbb{N}$ where $1 \leq i \leq \frac{q+1}{r+1}$, $1 \leq j \leq \frac{p+1}{r+1}, 1 \leq k \leq r-1$. By arguments of the proofs of Lemmas 3.10 and 3.12, any regular hexagon in the leftmost column of G is passed through by an element of L. The same is true for the regular hexagons in the bottom row, the rightmost column and the top row of G. Then, $L = \mathcal{K}_D^*$ holds for $r \geq 2$. We showed Theorem 3.15 in the case of $r \geq 2$.

Case 2: $r = 1$
$L = \{\text{the spur}\}$ holds. By Theorem 2.18, the spur passes through $(q, 1)_4$. If the spur passes around counterclockwise at $(q, 1)_4$, then $L = \mathcal{K}_D^*$ by Theorem 3.14. Assume that the spur passes around clockwise at $(q, 1)_4$. We show that there are no elements of $\mathcal{K}_D^* \setminus L$. We assume that there exists an element of $\mathcal{K}_D^* \setminus L$, denoted by T. By a similar argument of the proof of Theorem 2.18, T passes through at least one regular hexagon which has an intersection point of T and each side of ∂G. Let $(q, n_1)_4$ be a point which T passes through. Since the spur passes through $(q, 1)_4$, we see that $1 < n_1$. Let $(q, n_2)_4$ be the point which the spur passes through where $n_2 < n_1$ and $n_1 - n_2$ is minimum. For any point $(q, n_2')_4$ which the spur passes through, there exists the point $(q, n_1')_4$ which T passes through such that $n_1' - n_2' = n_1 - n_2$ by similar arguments of the proof of Lemma 3.10 and 3.12. Hence, the fact contradicts $r = 1$. Thus, there are no elements of $\mathcal{K}_D^* \setminus L$, i.e., $L = \mathcal{K}_D^*$ holds.

Therefore, D represents an r-component link. □

Theorem 3.16. *If $gcd(p+1, q+1) = 1$, then $r = 1$ and the spur traverses $(q, 1)$ counterclockwise. If $gcd(p+1, q+1) \neq 1$, then $r = gcd(p+1, q+1) - 1$ and the spur traverses $(q, 1)$ clockwise.*

Proof. Focus on the set of the broken segments composing the first half travel S_1 whose directions corresponds to the positive x-axis. Let u (v respectively) be the number of the regular hexagons that S_1 passes through in the top row (the rightmost column respectively) of G, i.e. $u, v \in \mathbb{N}$, $1 \leq u \leq q$, $1 \leq v \leq p$. Since the spur traverses $(q, 1)$ clockwise, by the sum of the lengths of the elements in the set, $(p+1)u - v = qv$ holds. Hence, $(p+1)u = (q+1)v$ holds. We note that $(u, v) \in \mathbb{N}^2$ is the minimal solution to the equation. Then, $(p+1)u = (q+1)v = lcm(p+1, q+1)$ holds. Furthermore, this fact together with $(p+1)(q+1) = lcm(p+1, q+1)gcd(p+1, q+1)$ shows that $gcd(p+1, q+1) = \frac{p+1}{v}$, $gcd(p+1, q+1) = \frac{q+1}{u}$. On the other hand, by an argument of the proof of Lemma 3.12, the regular hexagons in the leftmost column of G that S_1 passes through are located per distance of $r+1$. The same is true for regular hexagons in the bottom row, the rightmost column and the top row of G. Then, $\frac{p+1}{v} = \frac{q+1}{u} = r+1$ holds. These facts show that $r+1 = gcd(p+1, q+1)$ holds. Since $r \geq 1$, if $gcd(p+1, q+1) \neq 1$, then $r+1 = gcd(p+1, q+1)$ holds. Then, $gcd(p+1, q+1)$ is divided into the following two cases for the remainder of the proof of Theorem 3.16.

We assume $gcd(p+1, q+1) \neq 1$. Then, $r = gcd(p+1, q+1) - 1$ holds. If the spur traverses $(q, 1)$ counterclockwise, then $gcd(p+1, q+1) = 1$ holds by the proof of Theorem 3.14. Hence, if $gcd(p+1, q+1) \neq 1$, then $r = gcd(p+1, q+1) - 1$ and the spur traverses $(q, 1)$ clockwise.

We assume $gcd(p+1, q+1) = 1$. If the spur traverses $(q, 1)$ clockwise, then $(p+1)u = (q+1)v$ holds by the previous argument. Since $1 \leq v \leq p$, $gcd(p+1, q+1) \neq 1$ holds. This fact contradicts $gcd(p+1, q+1) = 1$. Then the spur on G traverses $(q, 1)$ counterclockwise. Hence, the CKD induced from G is a knot diagram by Theorem 3.14. This fact together with the definition of r shows that if $gcd(p+1, q+1) = 1$, then $r = 1$ and the spur traverses $(q, 1)$ counterclockwise. □

Example 3.17. For a CKD induced from a $5 \times q$ honeycomb grid, if $q = 5$, then $r = 5$; if $q = 6$, then $r = 1$; if $q = 8$, then $r = 2$; and if $q = 11$, then $r = 5$ as in Figure 20.

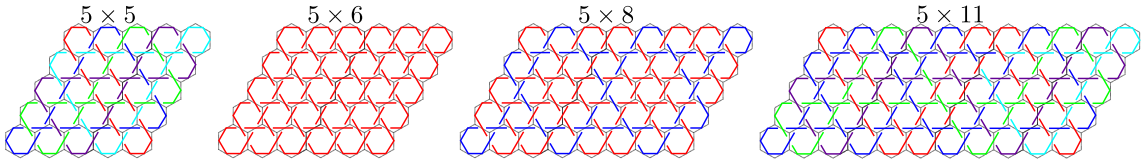

Figure 20: CKDs induced from $5 \times q$ honeycomb grids

Corollary 3.18. *If $p+1$ is a prime number, then $r = 1$ or $r = p$.*

Corollary 3.19. *Suppose that $p = 1$, then $r = 1$. Moreover, if q is even, then the spur traverses $(q, 1)$ counterclockwise, otherwise it traverses $(q, 1)$ clockwise.*

Corollary 3.20. *For $h \in \mathbb{N}$, if $q = h(p+1) - 1$, then $r = p$ and D represents a p-component link.*

We consider the opposite side of Corollary 3.20.

Proposition 3.21. *If $p \neq 1$ and D represents a p-component link, then $q \in \{h(p+1) - 1 \mid h \in \mathbb{N}\}$.*

Proof. By Theorem 3.15 and the assumption of Proposition 3.21, $r = p \geq 2$ holds. Then, by Theorem 3.14 and $r \geq 2$, the spur traverses $(q, 1)$ clockwise. Moreover, by the definition of T_k, T_k passes through $(q, k+1)_4$ $(1 \leq k \leq p-1)$. Let $(S_1, T_1, \ldots, T_{p-1})$ and $(S_2, S_1, T_1, \ldots, T_{p-1})$ be ordered sets. By Definition 2.14 and arguments of the proofs of Lemmas 3.10 and 3.12, the elements of $\mathcal{K}_D^*$ are lined up at the upper side of ∂G as follows: just $(S_1, T_1, \ldots, T_{p-1})$, or the sequence $(S_1, T_1, \ldots, T_{p-1})$, $(S_2, S_1, T_1, \ldots, T_{p-1}), \ldots, (S_2, S_1, T_1, \ldots, T_{p-1})$. Hence, $q \in \{h(p+1) - 1 \mid h \in \mathbb{N}\}$ holds. □

We assume $\gcd(p+1, q+1) \neq 1$. Then, $r = \gcd(p+1, q+1) - 1$ by Theorem 3.16. Let $1 \leq i' \leq \frac{q+1}{r+1} - 1$, $1 \leq j' \leq \frac{p+1}{r+1} - 1$, $1 \leq m \leq p$, $1 \leq n \leq q$. The closure of $G \setminus \bigcup ((i'(r+1), m) \cup (n, j'(r+1)))$ is the union of $r \times r$ honeycomb grids on G where the number of $r \times r$ honeycomb grids is $\frac{p+1}{r+1} \times \frac{q+1}{r+1}$. Let $1 \leq i \leq \frac{q+1}{r+1}$, $1 \leq j \leq \frac{p+1}{r+1}$. Let $G(i, j)$ be the $r \times r$ honeycomb grid composing the union located i-th from the left and j-th from the bottom on G. The broken segments of the spur of D of slope 0 and length q, and the broken segments of the spur of slope ∞ and length p divide G into $G(i, j)$ by Definition 2.14 and a similar argument of the proof of Lemma 3.12.

We extend deformations of a CKD in Figure 12 by applying the following Step 1 and Step 2. In Figures 21-23, $\partial G(i, j)$ is black, the interior of $G(i, j)$ shaded, and the replacing disks pink. Since the spur of D divides G into $G(i, j)$s, each crossing of D on $\partial G(i, j)$ involves the spur. Thus, the crossing is either a self crossing or a crossing of the spur and an element of the track of D. For

$k \in \mathbb{N}$ $(1 \leq k \leq r-1)$, let $T_k \in \mathcal{K}_D^*$ passing through the intersections of the regular hexagon $(q, p-r+1+k)$ and the right side of ∂G. By considering the shape of each element of $\mathcal{K}_D^*$ and the arrangement of $G(i,j)$, there exist two types of arrangements of crossings of D on $\partial G(i,j)$: one self crossing of the spur of D as (a) in Figure 21 and two adjacent crossings of the spur and T_k as (b) in Figure 21. Note that an arrangement (a) (an arrangement (b) respectively) in Figure 22 is composed of a combination of two copies of an arrangement (a) (an arrangement (b) respectively) in Figure 21. Then, the crossings in the exterior of $G(i,j)$ are self crossings as in Figures 21, 22 . Hence, for the two types of arrangements as in Figure 21, we define extensions of deformations of Figure 12 as Step 1 and Step 2. Moreover let $D(i,j)$ be the diagram on $G(i,j)$ obtained by Step 1 and Step 2.

Figure 21: The two types of arrangements of crossings of D on $\partial G(i,j)$

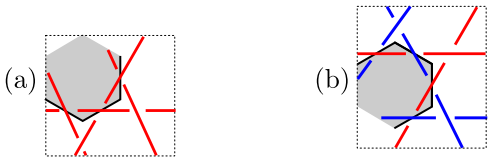

Figure 22: Arrangements are composed of figures in Figure 21.

Step 1 For any self crossing of the spur of D on $\partial G(i,j)$, take a small disk, and replace it with a new small disk as (a) in Figure 23.

Step 2 For any k, we focus on two adjacent crossings of the spur of D and T_k on $\partial G(i,j)$. Take a small disk including the crossings, and replace it with a new small disk as (b) in Figure 23.

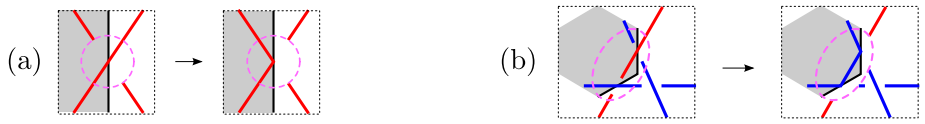

Figure 23: Deformations of a self crossing of the spur and two crossings of the spur and T_k

The diagram $D(i,j)$ is regarded as a CKD induced from $G(i,j)$ by the over/under information of the crossings of D. For any i, j, k, let $t_k^{D(i,j)} \in \mathcal{K}_{D(i,j)}^*$ passing through the intersection of the regular hexagon $(i(r+1)-1, (j-1)(r+1)+1+k)$ and the right side of $\partial G(i,j)$. By Step 1, Step 2 and the shapes of the elements of $\mathcal{K}_D^*$, the following theorem holds.

Theorem 3.22. *For any i, j, k, the spur of $D(i,j)$ ($t_k^{D(i,j)}$ respectively) corresponds to the spur of D (T_k respectively).*

The color of an element of $\mathcal{K}^*_{D(i,j)}$ obtained by Step 1, Step 2 coincides the color of the corresponding element of $\mathcal{K}^*_D$.

Corollary 3.23. $D(i,j) \parallel D(\frac{q+1}{r+1}, \frac{p+1}{r+1})$.

Proposition 3.24. *Any crossing of D on $G \setminus \bigcup G(i,j)$ is a self crossing.*

Example 3.25. Let D be the CKD induced from the 7×11 honeycomb grid. Then $r = 3$, $1 \leq i \leq \frac{11+1}{3+1}$, $1 \leq j \leq \frac{7+1}{3+1}$, $1 \leq k \leq 3-1$. The spur of $D(i,j)$ ($t_k^{D(i,j)}$ respectively) corresponds to the spur of D (T_k respectively) as in Figure 24. Any crossing of D on $G \setminus \bigcup G(i,j)$ is a self crossing.

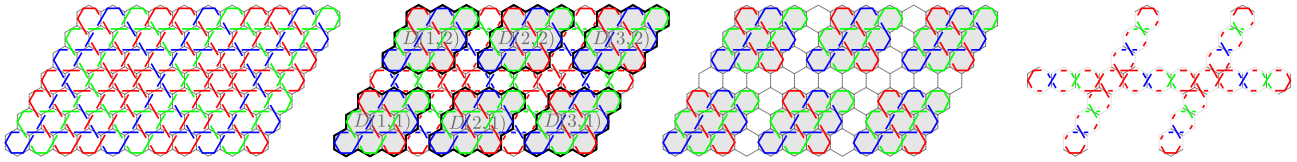

Figure 24: From left to right - D; the figure obtained from D by applying Step 1 and Step 2; $\bigcup D(i,j)$ on G; D on $G \setminus \bigcup G(i,j)$.

Corollary 3.26. *The number of the self crossings of the spur of D is $12(\frac{p+1}{r+1}-1)(\frac{q+1}{r+1}-1) + 2(\frac{p+1}{r+1}-1) + 2(\frac{q+1}{r+1}-1)$. The number of the self crossings of each element of the track of D is $\frac{p+1}{r+1} \cdot \frac{q+1}{r+1} + (\frac{p+1}{r+1}-1)\frac{q+1}{r+1} + \frac{p+1}{r+1}(\frac{q+1}{r+1}-1)$.*

Proposition 3.27. *For $h \in \mathbb{N}$, if $q = h(p+1)-1$, then $r = p$ and each element of $\mathcal{K}^*_D$ is the diagram of a trivial knot.*

Proof. By Corollary 3.20 and the assumption of Proposition 3.27, $r = p$. Hence we have $j = 1$ by $1 \leq j \leq \frac{p+1}{r+1}$. This fact together with Propositions 3.11, 3.24 and Corollary 3.23 shows that any crossing of any element of $\mathcal{K}^*_D$ is nugatory. Then, Proposition 3.27 holds. □

Theorem 3.28. *Any element of the track of D is uniquely determined up to plane ambient isotopy.*

Proof. Let $D_{p\times p}$ be the CKD induced from a $p \times p$ honeycomb grid. The number of the elements of $\mathcal{K}^*_{D_{p\times p}}$ is p by Theorems 3.15 and 3.16. By Proposition 3.11, each element of the track of $D_{p\times p}$ has one self crossing. The crossing of each element of the track consists of two line segments of slopes 0 and ∞. Thus, the over/under information of the crossing is uniquely determined. Hence, each element of the track of $D_{p\times p}$ is unique up to plane ambient isotopy.

For any $i,j,k \in \mathbb{N}$, the above argument and preliminaries of Theorem 3.22 show that $t_k^{D(i,j)}$ and $t_{k+1}^{D(i,j)}$ obtained from D is unique up to plane ambient isotopy, where $1 \leq i \leq \frac{q+1}{r+1}$, $1 \leq j \leq \frac{p+1}{r+1}$, $1 \leq k \leq r-1$. Moreover, for any $i',j,k \in \mathbb{N}$, by Theorem 3.22 and Proposition 3.24, $t_k^{D(i',j)}$ and $t_k^{D(i'+1,j)}$ are connected by a self crossing of T_k, where $1 \leq i' \leq \frac{q+1}{r+1}-1$. The crossing consists of two line segments of slopes -1 and 0. Then, the over/under information of the crossing is uniquely determined. Similarly, for any $i,j',k \in \mathbb{N}$, $t_k^{D(i,j')}$ and $t_k^{D(i,j'+1)}$ are connected by a self crossing of T_k, where $1 \leq j' \leq \frac{p+1}{r+1}-1$. The crossing consists of two line segments of slopes -1 and ∞. Then, the over/under information of the crossing is uniquely determined. Therefore, any element of the track of D is uniquely determined up to plane ambient isotopy. □

Proposition 3.29. *Any element of $\mathcal{K}_D^*$ is alternating.*

Proof. If $p = 1$ ($gcd(p+1, q+1) = 1$ respectively), D is a knot diagram by Corollaly 3.19 (Theorems 3.15 and 3.16 respectively). Thus, Proposition 3.29 holds. If $p \geq 2$, $gcd(p+1, q+1) \neq 1$ and $q = h(p+1)-1$ ($h \in \mathbb{N}$), then any element of $\mathcal{K}_D^*$ is alternating by Corollary 3.23, Propositions 3.11 and 3.24. In the remainder of this proof, suppose that $p \geq 2$, $gcd(p+1, q+1) \neq 1$ and $q \neq h(p+1)-1$ ($h \in \mathbb{N}$). Let P_K be a projection obtained from $K \in \mathcal{K}_D^*$.

First, we show that P_K has equilateral triangles (i.e. a triangle whose three sides are equal in length) and hexagons on the interior of G. Then, K consists of the broken segments each with slope -1, 0 or ∞. For any broken segment, take the straight line that includes itself.

Assume K is an element of the track. The distance between any pair of parallel and adjacent broken segments of K with length greater than $\frac{1}{2}$ on G is $r+1$ by an argument of the proof of Lemma 3.10. Fix a broken segment of K of slope 0 (∞, -1, respectively) and length greater than $\frac{1}{2}$, and let X_t (Y_t, Z_t, respectively) be the set of infinite parallel straight lines which are arranged per distance of $r+1$ on the plane, where the set includes the straight line obtained from the broken segment. Three lines - one from each of X_s, Y_t, and Z_t - form an equilateral triangle. Six lines - two from each set - form a hexagon. Hence, $X_t \cup Y_t \cup Z_t$ divides the plane into the equilateral triangles and the hexagons. Then, P_K has the equilateral triangles and the hexagons on the interior of G.

Assume K is the spur. The parallel and adjacent straight lines obtained from broken segments of K alternate between distance of r and 1 by an argument of the proof of Lemma 3.12. Fix a broken segment of $S_1 \subset K$ with length greater than $\frac{1}{2}$. The image on G obtained from the fixed broken segment of S_1 of slope 0 (∞, -1, respectively) by the parallel translation of -1 along the y-axis (x-axis, x-axis respectively) is the broken segment of $S_2 \subset K$ by Lemma 3.12. Let X_s (Y_s, Z_s, respectively) be the set of infinite parallel straight lines which are arranged per distance of $r+1$ on the plane, where the set includes the straight line obtained from the fixed broken segment of slope 0 (∞, -1, respectively). Let X_s' (Y_s', Z_s' respectively) be the set obtained by translating X_s (Y_s, Z_s respectively) by -1 along the y-axis (x-axis, x-axis respectively). Hence, $X_s \cup X_s' \cup Y_s \cup Y_s' \cup Z_s \cup Z_s'$ divides the plane into the equilateral triangles and the hexagons as in Figure 25. Then, P_K has the equilateral triangles and the hexagons on the interior of G.

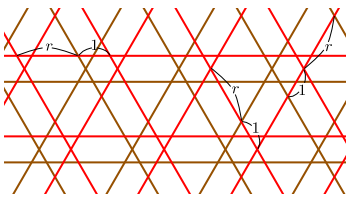

Figure 25: Elements of $X_s \cup Y_s \cup Z_s$ ($X_s' \cup Y_s' \cup Z_s'$ respectively) are depicted in red (brown respectively)

Second, we show that any crossing of K corresponds to a vertex of the polygons on the interior of G. Assume K is an element of the track. The shape of K is recognized by Corollaries 3.23, 3.26, Theorem 3.22 and Proposition 3.24. Recall that there exists just one crossing of $t_k^{D(i,j)}$ on $G(i,j)$ for $1 \leq i \leq \frac{q+1}{r+1}$, $1 \leq j \leq \frac{p+1}{r+1}$. For any $D(i,j)$ ($(i,j) \neq (1, \frac{p+1}{r+1}), (\frac{q+1}{r+1}, 1)$) and k, the crossing of $t_k^{D(i,j)}$ corresponds to the vertex of at least one equilateral triangle on the interior of G. We checked $\frac{p+1}{r+1} \cdot \frac{q+1}{r+1} - 2$ crossings. The self crossings on $G \setminus \bigcup G(i,j)$ correspond to the remaining vertices of

the equilateral triangle. We checked $(\frac{p+1}{r+1}-1)\frac{q+1}{r+1}+\frac{p+1}{r+1}(\frac{q+1}{r+1}-1)$ crossings. By the assumption of p and q, there are two or more broken segments of K of slope -1 and length greater than $\frac{1}{2}$ on G. The same is true for broken segments of slope 0 or ∞ and length greater than $\frac{1}{2}$ on G. Recall that the distance between any pair of parallel and adjacent broken segments of K with length greater than $\frac{1}{2}$ on G is $r+1$. Then, for $(i,j)=(1,\frac{p+1}{r+1}),(\frac{q+1}{r+1},1)$, K has two broken segments that passes through $G(i,j)$ of slope -1, and $t_k^{D(i,j)}$ has two broken segments of slopes 0 and ∞ and length greater than $\frac{1}{2}$ by the shape of $D(i,j)$. The crossing of $t_k^{D(i,j)}$ corresponds to the crossing of K consisting of the broken segments of slopes 0 and ∞ by Theorem 3.22 and Corollary 3.23. By the assumption of p and q, there exists the broken segment of K of slope 0 and length greater than $\frac{1}{2}$ on G at a distance of $r+1$ from the broken segment of K of slope 0. The same is true for the broken segment of slope ∞ on G. The straight lines including these six broken segments form a hexagon on the interior of G. Thus, for $(i,j)=(1,\frac{p+1}{r+1}),(\frac{q+1}{r+1},1)$, the crossing of $t_k^{D(i,j)}$ corresponds to the vertex of the hexagon on the interior of G. We checked two crossings. Then, we checked all crossings of K by Corollary 3.26. Hence, any crossing of K corresponds to a vertex of the equilateral triangles or a vertex of the hexagons on the interior of G in this case.

Assume K is the spur. The shape of K is recognized by Corollaries 3.23, 3.26, Theorem 3.22 and Proposition 3.24. Any crossing of K is in the closure of $G\setminus\bigcup G(i,j)$ by Proposition 3.11 and Corollary 3.23. Any $G(i,j)$ is obtained by dividing G by the broken segments of K of slope 0 and length q, and the broken segments of K of slope ∞ and length p. Then, the union of the straight lines obtained from the broken segments of K of slope -1 and the straight lines obtained from the broken segments that divide G forms the equilateral triangles and the regular hexagons with side length $\frac{1}{2}$ on the interior of G. Let A be the set of the crossings of K each of which is corresponding to a vertex of the equilateral triangles. We checked $12(\frac{p+1}{r+1}-1)(\frac{q+1}{r+1}-1)$ crossings. Let B be the set of the crossings of K not in A. Since any element of B is not in A and on $\partial G(i,j)$ having an intersection with ∂G, any element of B corresponds to a vertex of the equilateral triangles with side length $r-\frac{1}{2}$ on the interior of G. We checked $2(\frac{p+1}{r+1}-1)+2(\frac{q+1}{r+1}-1)$ crossings. Then, we checked all crossings of K by Corollary 3.26. Hence, any crossing of K corresponds to a vertex of the equilateral triangles on the interior of G in this case.

Finally, we show that the crossings of K corresponding to the vertices of a polygon on the interior of G are "locally alternating", in order to show that K is alternating. Take a compact region intersecting with a diagram of a link on the plane. The intersection points of the boundary of the region and the diagram are transverse double points. The intersection of the region and the diagram is called *the restricted diagram by the region*. We say that the restricted diagram by the region is *locally alternating* if the over/under information of the crossings on every segment in the restricted diagram appears alternately. For any polygon of P_K on the interior of G, take a neighborhood of the polygon that is not including a vertex of another polygon. The neighborhood corresponds to the compact region intersecting K. If the restricted diagrams by the neighborhoods are locally alternating, then K is alternating because any crossing of K corresponds to a vertex of the polygons on the interior of G. Hence, the restricted diagram by the neighborhood is locally alternating because the over/under information of the crossings on every segment in the restricted diagram by the neighborhood appears alternately by the slopes of the broken segments of K. Therefore, K is alternating.

In all cases, any element of $\mathcal{K}_D^*$ is alternating. □

Example 3.30. Let D be the CKD induced from the 7×11 honeycomb grid as in Figure 8. Then,

the spur passes through $(11, 1)$. Moreover, the elements of the track ($K_2, K_3 \in \mathcal{K}_D^*$) are unique up to plane ambient isotopy. Any element of $\mathcal{K}_D^*$ is alternating.

Acknowledgment

We sincerely thank the anonymous referee for their careful reading and helpful comments, which greatly improved this manuscript.

References

[1] P. R. Cromwell, "Celtic knotwork: mathematical art", *Math. Intelligencer, 15 no 1* (1993), 36-47.

[2] P. R. Cromwell, "The distribution of knot types in Celtic interlaced ornament", *J. Mathematics and the Arts 2* (2008), 61-68.

[3] G. Fisher & B. Mellor, "On the Topology of Celtic Knot Designs", *Bridges Mathematical Connections in Art, Music, and Science* (2004), 37-44.

[4] Y. Funakoshi, "Animations based on knot theory for drawing Celtic knot projection of $p \times q$ square grid and $p \times q$ honeycomb grid", *The annals of Gifu Shotoku Gakuen University. Faculty of Education, 63 (2024)*, 21-40, Japanese.

[5] L. H. Kauffman, "State Models and the Jones Polynomial", *Topology 26* (1987), 395-407.

[6] A. Kawauchi, *A Survey of Knot Theory*, Birkhäuser, Basel (1996).

[7] A. Meehan, *Celtic Design, Knotwork, The Secret Method of the Scribes*, Thames and Hudson (1991).

[8] K. Murasugi, "The Jones Polynomial and Classical Conjectures in Knot Theory", *Topology 26* (1987), 187-194.

[9] M. B. Thistlethwaite, "A Spanning Tree Expansion of the Jones Polynomial", *Topology 26* (1987), 297-309.

[10] Code.org, CSTA, and ECEP Alliance. *2024 State of Computer Science Education*. Code.org Advocacy Coalition, 2024.

[11] Perales, F. J., & Aróstegui, J. L. (2024). The STEAM approach: Implementation and educational, social and economic consequences. *Arts Education Policy Review*, 125(2), 59-67.